J Neuropathol Exp Neurol
Vol. 65, No. 10
October 2006
pp. 1022–1030

ORIGINAL ARTICLE

Latency of α-Herpes Viruses Is Accompanied by a Chronic Inflammation in Human Trigeminal Ganglia But Not in Dorsal Root Ganglia

Katharina Hüfner, MD, Tobias Derfuss, MD, Simone Herberger, MD, Kishiko Sunami, MD, Steven Russell, MD, Inga Sinicina, MD, Viktor Arbusow, MD, Michael Strupp, MD, Thomas Brandt, MD, FRCP, and Diethilde Theil, DVM

Abstract

The immune response to latent herpesvirus infections was compared in human trigeminal ganglia (TG) and dorsal root ganglia (DRG) of 15 dead individuals. On the basis of our previous findings, we hypothesized that T-cells would be attracted to sensory neurons latently infected with herpes simplex virus type 1 (HSV-1), but not to those harboring latent varicella zoster virus (VZV). We showed that the TG contain a positive hybridization signal for HSV-1 latency-associated transcript (LAT), whereas the DRG from the same individuals lack detectable LAT. In contrast, immunohistochemistry revealed that latent VZV protein 62 stained positive in the vast majority of all tested TG and DRG. T-cell infiltrates prominently surrounded individual neurons in the TG but not in the DRG. TaqMan polymerase chain reaction also showed higher expression of CD8 and RANTES transcripts in the TG versus DRG. Only the infiltrates in the TG, but not in the DRG, produced RANTES at the protein level. Because it has been shown that RANTES protein is produced only after T-cell receptor stimulation, we assume that T-cell infiltration is associated with antigen recognition in the TG but not in the DRG.

Key Words: Dorsal root ganglia, Herpes simplex virus type 1, RANTES, T-cells, Trigeminal ganglia, Varicella zoster virus.

INTRODUCTION

Most infectious diseases that originate from sensory ganglia develop from a latent infection with α-herpesviruses: herpes simplex type-1 (HSV-1) and varicella zoster virus (VZV). These viruses are closely related (1–4). They both show a highly homologous DNA sequence and a linear organization of the viral genome, replicate in similar ways, and in particular have the ability to establish lifelong latent infections in sensory neurons. Both viruses can reactivate from a latent state in the neural nuclei, undergo anterograde axonal transport to the site of primary infection (HSV-1) or to the respective dermatome (VZV), and replicate intensely, causing epithelial damage and pain. The most common syndromes are *herpes labialis,* usually recurrent and caused by repeated reactivation of HSV-1, and *herpes zoster,* a painful disorder usually caused by a single reactivation of VZV, which can involve postherpetic neuralgia as a serious sequela.

Although similar, these viruses are different in their clinical manifestations and their reactivation. These differences might be associated with distinct patterns of latency. The latent HSV-1 genome is classically considered to be transcriptionally silent, except for a family of latency-associated transcripts (LATs), which are not known to be translated into proteins (5, 6). However, recent evidence from experiments in mice suggests that a limited array of HSV-1 proteins might be produced during latency, and these could be responsible for attracting and retaining HSV-1-specific T-cells within the ganglion (7, 8).

In contrast, viral RNA and protein corresponding to genes 21, 29, 62, and 63 have been consistently detected during VZV latency in humans (9, 10). It has never been shown whether these proteins have an antigenic activity in vivo, because there is no animal model for the human disease caused by VZV, and it is not possible to experimentally reactivate latent VZV (11). Hence, it is essential to analyze molecular aspects of VZV latency on human autopsy material from healthy individuals.

In a previous study, we identified persistent T-cell infiltrates in human trigeminal ganglia (TG) latently coinfected with HSV-1 and VZV or infected with only latent HSV-1 (12). Fewer T-cells were detected in the TG of an individual infected only with VZV than in those infected with HSV-1 alone or coinfected with both viruses. These findings as well as data from the HSV-1 animal model led us to hypothesize that T-cells would more readily be attracted to neurons that

From the Department of Neurology (KH, TD, SH, KS, SR, VA, MS, TB, DT), Klinikum Grosshadern, Ludwig-Maximilians University, Munich, Germany; Max Planck Institute of Psychiatry (TD), Munich, Germany; the Department of Otolaryngology and Head and Neck Surgery (KS), Osaka City University Graduate School of Medicine, Osaka, Japan; the Department of Neurosurgery (SR), New York University School of Medicine, New York, NY; and the Department of Legal Medicine (IS), Ludwig-Maximilians University, Munich, Germany.

Send correspondence and reprint requests to: Dr. Diethilde Theil, Department of Neurology, Klinikum Grosshadern, Marchioninistr. 23, 81377 Munich, Germany; E-mail: dtheil@brain.nefo.med.uni-muenchen.de

K. Hüfner and T. Derfuss contributed equally to this study.

This work was supported by the Deutsche Forschungsgemeinschaft (TH 894/1-1) and Friedrich-Baur Stiftung.

TABLE 1. Characteristics of the 15 Subjects Analyzed in This Study

Subject	Age/Gender	Cause of Death	Number of Tested DRGs	Time Until Autopsy	GAPDH PCR Cycles
1	60 years, F	Unclear, found dead in bed	1	24 h	13.8
2	90 years, F	Heart failure	1	29 h	12.2
3	63 years, M	Electric shock	1	24 h	13.8
4	52 years, F	Myocardial infarction	1	15 h	15.0
5	39 years, F	Dissecting aorta aneurysm	3	19 h	16.0
6	17 years, M	Hanging	3	17 h	16.0
7	12 years, M	Hanging	4	21 h	18.7
8	48 years, M	Heart failure	1	5 h	14.7
9	85 years, F	Stabbing	1	6 h	13.4
10	25 years, M	Stabbing	6	29 h	18.7
11	26 years, M	Stabbing	3	29 h	15.7
12	43 years, F	Car accident	4	20 h	16.7
13	52 years, M	Heart failure	3	13 h	16.2
14	44 years, M	Craniocerebral injury	3	19 h	11.8
15	63 years, M	Car accident	2	25 h	17.1

The number of the thoracic DRG tested from each subject as well as the interval between death and autopsy are shown. The number of cycles necessary before a GAPDH signal became discernible using quantitative PCR is shown in the last column. The number of PCR cycles inversely correlates with the quality of the starting RNA. There was no correlation between the time until autopsy and the quality of RNA.

DRG, dorsal root ganglia; PCR, polymerase chain reaction.

harbor latent HSV-1 than to those harboring latent VZV (7, 13, 14). If this hypothesis proves true, it will supply evidence that the immune response to latent VZV is limited despite abundant protein expression during latent infection.

To determine which of the 2 latent virus infections is responsible for the persistent immune response, we assessed the TG and dorsal root ganglia (DRG) of 15 cadavers for the presence of T-cells and for the presence of RANTES as a marker of an ongoing immune response (15). Beforehand, all TG and DRG were examined for the presence of latent HSV-1 and VZV. The differential presence of latent HSV-1 and VZV in the TG and DRG allowed us to assess if the latent viruses varied in their capacity to cause T-cell infiltrations.

MATERIALS AND METHODS

Samples

The use of autopsy samples for the present study was approved by the Ethics Committee of the Medical Faculty of the Ludwig-Maximilians University of Munich. TG and the corresponding DRG at one or more levels were removed 5 to 29 hours after death from 15 subjects whose ages ranged from 12 to 90 years. The causes of their death were mainly related to trauma (Table 1). The subjects had no lesions suggestive of an active orolabial herpes infection. For frozen sections, ganglia were embedded in Tissue Tek compound (Sakura, Zoeterwoude, The Netherlands) and stored on dry ice at –70°C until use. For paraffin processing, the tissue was first fixed in 4% buffered paraformaldehyde for 48 hours. Frozen sections were 8-μm thick and paraffin sections were 4-μm thick. The sections were mounted on positively charged slides (SuperFrost/Plus; Menzel, Braunschweig, Germany). Several tissue sections from the ganglia were stained with hematoxylin and eosin (H&E; Sigma, Deisenhofen, Germany) for light microscopy examination.

Latency-Associated Transcript In Situ Hybridization

LAT in situ hybridization was performed as described previously (12). The hybridized antisense LAT probes were

TABLE 2. Quantification of Latency-Associated Transcripts, CD8, and RANTES Transcripts in TG and DRG by Quantitative Reverse Transcriptase–Polymerase Chain Reaction

Subject	LAT TG	LAT DRG	IF CD8TG/ DRG	IF RANTESTG/ DRG	Number of Tested DRG
1	33	0	0.7	1.1	1/1
2	5	0	0.5	3.3	1/1
3	3	0	3.5	6.3	1/1
4	512	0	2.2	102.4	1/1
5	272	0	2.6	12.4	2/3
6	ND	0	2.2	13.5	2/3
7	2	0	1	2.1	4/4
8	17	0	ND	ND	0/1
9	820	0	1	7.3	1/1
10	125	0	30	49.1	4/6
11	1	0	1	1.7	2/3
12	2	0	2.1	7.7	4/4
13	1	0	63.3	124.1	2/3
14	4	0	4.4	11	3/3
15	44	0	13	8.5	2/2

The relative amount of LAT transcript compared with GAPDH in the TG is shown in the first column. At least one DRG from each individual was tested by SYBR green PCR and all others by conventional LAT reverse transcriptase–PCR. No LAT transcript could be found in all tested DRG (second column). For comparison of RANTES and CD8 expression in the TG and DRG, an induction factor (IF) has been calculated by dividing the relative transcript number in the TG and the respective DRG. For the DRG, the mean IF of all DRG analyzed for one case was used. The number of DRG analyzed for the presence of CD8 transcript and RANTES is also listed.

TG, trigeminal ganglia; DRG, dorsal root ganglia; LAT, latency-associated transcript; ND, not done; PCR, polymerase chain reaction.

detected using alkaline phosphate conjugated antidigoxigenin antibodies included in the DIG Nucleic Acid Detection Kit (Roche Molecular Biochemicals, Mannheim, Germany) and 5-bromo-4-chloro-3-indolyl phosphate/nitro blue tetrazolium (NBT; Roche Molecular Biochemicals).

Herpes Simplex Virus Type 1 Nested DNA Polymerase Chain Reaction and Latency-Associated Transcript Reverse Transcriptase–Polymerase Chain Reaction

DNA was isolated from the DRG with the Qiagen DNA Extraction Kit (Qiagen, Hilden, Germany) or Trizol (Life Technologies, Karlsruhe, Germany) according to the manufacturer's instructions using aerosol-free pipette tips. Both methods yielded similar amounts and purity of DNA. Preparations of DNA, first round of nested polymerase chain reaction (PCR), and second round of nested PCR were all done in separate laboratory rooms. Nested PCR was carried out with the primers described by Aurelius et al (16). Thirty cycles were run for each round. Several negative water controls were used in each reaction and an HSV-1 boiled virus culture suspension (provided by Dr. Haas, Max von Pettenkofer-Institut, Munich, Germany) was used as a positive control.

RNA was prepared from the TG of one side and DRG with Trizol (Life Technologies) or RNeasy Mini Kit (Qiagen) according to the manufacturer's instructions using aerosol-free pipette tips. RNA was reverse transcribed and to ensure the integrity of the RNA subsequent PCR with primers specific for β-actin cDNA was performed as described previously (17). LAT PCR was performed using primers and conditions described elsewhere (18).

Immunohistochemistry

Immunohistochemical stainings were done with primary antibodies against T-cell markers: rabbit anti-human CD3 (1:1000) and mouse anti-human CD8 (1:80; DAKO, Hamburg, Germany). For the detection of VZV-specific

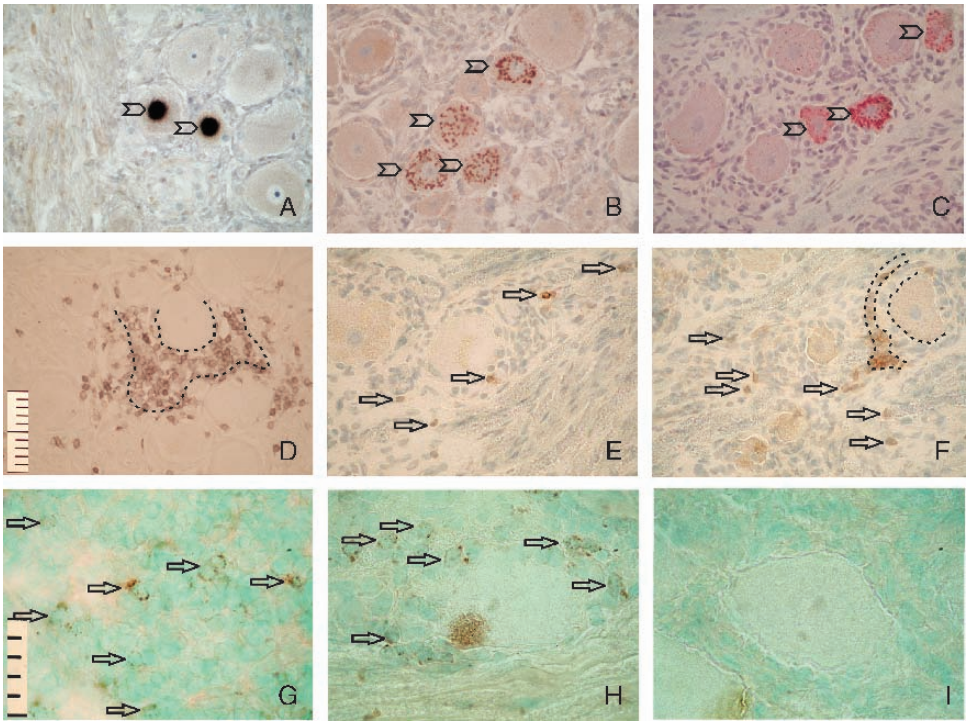

FIGURE 1. Comparison of the herpes simplex virus type 1 and varicella zoster virus (VZV) latency and the immune cell infiltration in human trigeminal ganglia (TG) and dorsal root ganglia (DRG). **(A)** Positive latency-associated transcript (LAT) in situ hybridization signal (dark blue nuclei [NBT]) on a TG section. The 2 LAT-positive cells are marked by arrowheads. None of the DRG exhibited such staining (not shown). **(B)** VZV protein 62 in the TG (brown, DAB, marked by arrowheads), and similarly **(C)** VZV protein 62 in the DRG (red, ACE; marked by arrowheads). **(D)** Numerous CD3+ T-cells (brown cells, DAB) are seen in direct contact with a neuron in the TG (dashed inner line encircles the neuron; dashed outer line encircles the T-cell infiltrates). **(E)** Only a few CD3+ T-cells are scattered among nerve fibers in the DRG (brown cells, DAB; marked by arrows). **(F)** A rare grouping of CD3+ T-cells was seen in a few DRG (brown cells, DAB; arrows) (dashed inner line encircles the neuron; 2 outer lines demarcate the infiltrating T-cells). The grouped T-cells in the DRG were not in close contact with the neuron. They are separated by resident cells, which appear to be satellite cells. **(G)** A tonsil section shows several T-cells positive for RANTES (brown staining, DAB; aggregates marked by arrows). **(H)** In the TG, RANTES is expressed in the infiltrating cells with sparse cytoplasm, which histologically resemble T-cells (brown staining, DAB; aggregates marked by arrows), whereas no RANTES was detectable in DRG **(I)**. Micrographs were taken at a magnification of 400x for the first 2 rows and 1,000x for the third row. The size of the scale bar in **(D)** is 0.1 mm; the subdivisions are 0.01 mm apart; in **(G)** the size is 0.05 mm and the subdivisions are 0.01 mm apart.

antigen, mouse anti-VZV protein 62 (1:100; Chemicon, Hofheim, Germany), and for detection of the chemokine RANTES a goat anti-RANTES antibody (1:20; R&D Systems, Wiesbaden, Germany) were applied. A previously described protocol was used (12). In brief, frozen tissue sections were thawed, dried at 37°C for 15 minutes, fixed in acetone for RANTES stainings or in 4% buffered paraformaldehyde (all other stainings) for 10 minutes, and then washed in phosphate-buffered saline (PBS). Paraffin sections were dewaxed, rehydrated, and then washed in PBS. For the immunostainings with anti-CD3 antibodies, paraffin sections were treated with antigen-retrieval solution (DAKO) for 5 minutes. Frozen and paraffin sections were then sequentially incubated with 0.5% to 3% hydrogen peroxide for 10 minutes, 5% normal rabbit serum, or 5% normal goat serum for 30 minutes. The diluted primary antibodies were applied to the sections and left to incubate overnight at 4°C. Afterward, tissue sections were incubated for 30 minutes with biotinylated rabbit anti-mouse IgG antibody (1:300; DAKO), biotinylated rabbit anti-goat IgG antibody (1:800; DAKO), or biotinylated goat anti-rabbit IgG antibody (1:300; DAKO). The sections were incubated with peroxidase-conjugated streptavidin or AB complex (DAKO) for 30 minutes, followed by a final wash, and then incubated with diaminobenzidine (DAB; DAKO) or 3-amino-9 ethyl carbazole (ACE; DAKO) for up to 10 minutes. The prevalence of CD3, CD8, VZV62, and RANTES antigen was assessed in the TG and the DRG of each individual. The TG of one side was evaluated by immunohistochemistry and the TG of the other side was used for quantitative real-time reverse transcriptase– (RT) PCR.

Quantitative Real-Time Reverse Transcriptase–Polymerase Chain Reaction

Primers and TaqMan probes for the chemokine RANTES (12) and the T-cell marker CD8 (19) were used as described previously. These primers were intron spanning. Cyclophilin D primers and TaqMan probes were purchased from Applied Biosystems (Foster City, CA). TaqMan and SYBR green PCR were performed using the GeneAmp 5700 Sequence Detection System (Applied Biosystems). Data were analyzed with GeneAmp5700 SDS software (Applied Biosystems). The relative transcript number was calculated from the formula $2^{-\Delta Ct} \times 10^5$, where ΔCt stands for the difference between the threshold cycle number of the housekeeping gene and the respective gene of interest. For quantification of LAT transcripts, the QuantiTect SYBR green PCR kit (Qiagen) was used and the previously described primers (17). The results of the SYBR green PCR were normalized to the housekeeping gene GAPDH. An induction factor was calculated by dividing the relative transcript number in the TG and the respective DRG (Table 2) to compare RANTES and CD8 expression in the TG and DRG.

RESULTS

Distribution of Herpes Simplex Virus Type 1 in Human Trigeminal Ganglia and Dorsal Root Ganglia

HSV-1 LAT was detected in the TG of 12 of 15 tested individuals by in situ hybridization (Fig. 1A). LAT+ neurons were mainly found in clusters. When LAT Taqman PCR was

TABLE 3. Frequency and Distribution of Herpes Simplex Virus Type 1, Varicella Zoster Virus, and CD3+ T-Cells in Trigeminal Ganglia and Dorsal Root Ganglia

Subject	Percent of VZV-Positive Neurons in TG	Percent of VZV-Positive Neurons in DRG	Number of VZV-Positive DRG	Number of HSV-1-Positive DRG	Number of CD3 in TG	Number of CD3 in DRG
1	8	14	1/1	1/1	>100	11
2	15	39	1/1	0/1	>100	5
3	9	17	1/1	0/1	59	7
4	21	14	1/1	0/1	62	22
5	0	6	1/3	0/3	>100	18
6	17	33	3/3	1/3	>100	30
7	0	13	3/4	0/4	17	6
8	5	15	1/1	1/1	>100	18
9	6	24	1/1	1/1	47	17
10	0	12	6/6	2/6	>100	24
11	17	20	3/3	0/3	42	20
12	18	36	2/4	0/4	72	10
13	12	14	3/3	1/3	93	24
14	8	20	3/3	1/3	>100	22
15	11	6	2/2	2/2	>100	25

VZV-positive neurons are given as a percentage of all neurons evaluated in 3 fields of view at a magnification of 400×. Between 20 and 120 neurons were analyzed for each ganglion. For reasons of simplicity, the mean number of positive neurons of all positive ganglia is given for the DRG. The third column indicates the number of VZV-positive DRG using immunohistochemistry; the number of positive DRG of all tested DRG per individual is given. Results of the nested HSV-1 polymerase chain reaction are shown in the fourth column; the number of positive DRG out of all tested DRG per individual is given. The fifth and sixth columns show the CD3+ T-cell counts in the TG and the DRG. The T-cell number was determined in 3 fields of view at a magnification of 400×.

VZV, varicella zoster virus; TG, trigeminal ganglia; DRG, dorsal root ganglia; HSV-1, herpes simplex virus type 1.

used, all tested TG were positive, including those that were negative by in situ hybridization. LAT transcript numbers varied among individuals by a factor of 1000 (Table 2). In contrast, all 37 DRG were negative for LAT when in situ hybridization, LAT RT-PCR, or LAT TaqMan PCR were used. HSV-1 DNA was detected in 10 of 37 DRG through nested PCR.

Distribution of Varicella Zoster Virus Protein 62 in Human Trigeminal Ganglia and Dorsal Root Ganglia

VZV protein 62 was present in 12 of 15 TG (Fig. 1B; Table 3) and in 32 of 37 DRG (Fig. 1C; Table 3). All of the 15 individuals tested in this study had at least one DRG positive for VZV, even those with TG that was negative for VZV. When several DRG from one subject were analyzed, not all DRG were consistently positive or negative for VZV protein 62 antigen (Table 3). Positive VZV protein 62 neurons were randomly distributed in the entire TG and DRG and the staining was confined to only the cytoplasm.

For quantification, 3 fields of view with VZV-positive neurons were selected, and the percentage of protein 62-positive neurons was determined. The percentage of VZV-positive neurons in DRG was 16.7 ± 1.9% (mean ± standard error of mean [SEM]) and in TG, 12.3 ± 1.5% (mean ± SEM). In general, VZV-positive cells were present in larger numbers in the DRG than in the TG, but this did not reach statistical significance.

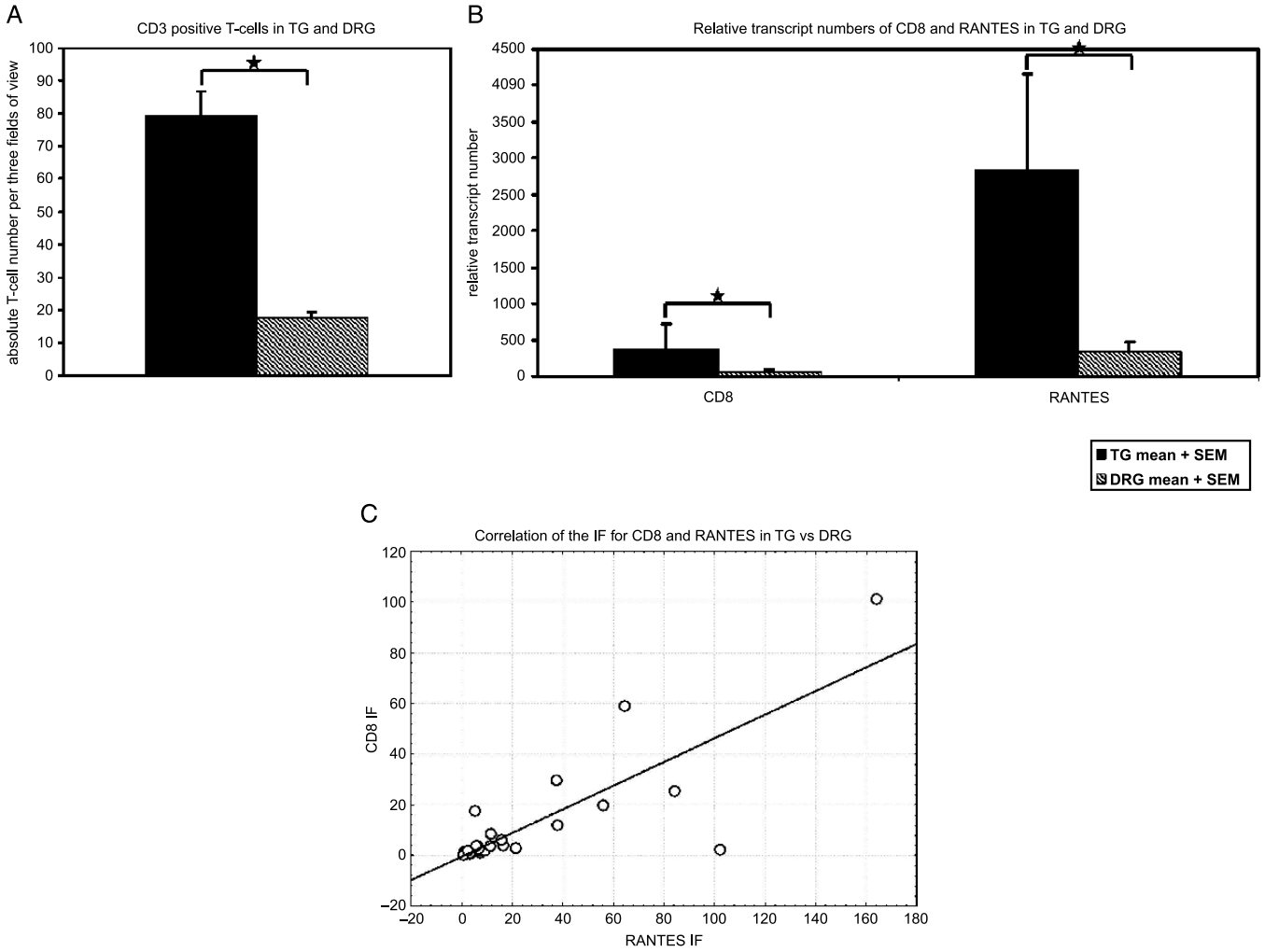

FIGURE 2. Quantification and comparison of CD3+ T-cells and CD8 and RANTES transcripts in the trigeminal ganglia (TG) versus dorsal root ganglia (DRG). **(A)** Assessment of the number of CD3+ T-cells in the TG (black bars) and DRG (gray bars) by immunohistochemistry. CD3+ T-cell numbers were significantly higher in the TG than in the DRG (Mann-Whitney U test, $p < 0.00001$). **(B)** Transcript levels of CD8 and RANTES in the TG (black bars) and DRG (gray bars). The y-axis depicts the relative transcript number normalized to the housekeeping gene (cyclophilin). Significantly lower levels of CD8 and RANTES transcripts were found in the DRG (Mann-Whitney U test, $p < 0.01$ and $p < 0.001$). The asterisk indicates statistically significant differences. **(C)** Correlation of CD8 and RANTES transcripts. For comparison of RANTES and CD8 expression in the TG and DRG, an induction factor (IF) was calculated by dividing the relative transcript number in the TG and the respective DRG. The induction factor for CD8 and RANTES were plotted for each individual. There was a statistically significant correlation between the accumulation of CD8 and RANTES transcripts in the TG versus DRG (Spearman rank order correlation, $r = 0.79$, $p < 0.001$).

TABLE 4. Overview of the Individual Ganglia Analyzed in This Study

Case	VZV Percent + Neurons	LAT Relative Transcript Number	HSV-1 DNA + Ganglia	CD3 Absolute Number	CD8 Relative Transcript Number	RANTES Relative Transcript Number
1Th3	14	0	1	11	12	191
1TG	8	33	1	>100	8	209
2Th3	39	0	0	5	25	140
2TG	15	5	1	>100	13	468
3Th4	17	0	0	7	13	141
3TG	9	3	1	59	45	889
4Th9	14	0	0	22	11	9
4TG	21	512	1	62	24	922
5Th4	0	0	0	7	15	100
5Th5	6	0	0	29	6	50
5Th6	0	0	0	18	ND	ND
5TG	0	272	1	>100	22	825
6Th5	39	0	0	15	8	46
6Th6	35	0	0	36	14	178
6Th7	27	0	1	38	ND	ND
6TG	17	ND	1	>100	22	987
7Th1R	20	0	0	8	6	49
7Th2R	0	0	0	4	20	87
7Th1L	10	0	0	11	5	93
7Th5L	9	0	0	1	9	33
7TG	0	2	1	17	7	112
8Th4R	15	0	1	18	ND	ND
8TG	5	17	1	>100	ND	ND
9Th3R	24	0	1	17	7	64
9TG	6	820	1	47	7	465
10Th3R	3	0	0	15	0	53
10Th4R	12	0	1	18	3	61
10Th5R	11	0	0	22	ND	ND
10Th3L	6	0	0	53	5	90
10Th5L	15	0	0	0	ND	ND
10Th6L	23	0	1	20	2	91
10 TG	0	125	1	>100	59	3420
11Th4R	19	0	0	12	ND	ND
11Th5R	17	0	0	31	872	2816
11Th6R	25	0	0	17	76	831
11TG	17	1	1	42	135	2164
12Th4L	40	0	0	11	5	51
12Th5L	32	0	0	8	5	46
12Th3R	0	0	0	15	4	53
12Th5R	0	0	0	6	6	39
12TG	18	2	1	72	10	359
13Th3L	6	0	0	4	ND	ND
13Th4L	24	0	0	13	12	146
13Th5L	13	0	1	56	3	75
13TG	12	1	1	93	304	12299
14Th1L	16	0	0	30	5	113
14Th2L	15	0	1	24	3	41
14Th3	29	0	0	11	5	57
14TG	8	4	1	>100	18	649
15Th2L	4	0	1	31	268	2977
15Th3L	7	0	1	19	560	1398
15TG	11	44	1	>100	4703	16042

Prominent T-Cell Infiltration in the Trigeminal Ganglia But Not the Dorsal Root Ganglia

An abundant infiltration with CD3+ T-cells mainly of the CD8+ phenotype was detected in the TG. In the majority of the TG, the T-cells were clustered around neurons (Fig. 1D). In contrast, only a modest number of CD3+ T-cells was present in the DRG; and they were randomly scattered over the entire DRG: between the neurons, in the nerve fibers, and in the connective tissue. In contrast to the TG, the T-cells were rarely found in larger aggregates (Fig. 1E) or in close proximity to the neurons and they were not in direct contact with the neurons (Fig. 1F, dashed line). The infiltrating CD3+ T-cells were counted in 3 fields of view that showed T-cell clustering or accumulation. If clustering or accumulation was not present, T-cells in 3 randomly selected fields of view were counted. The number of infiltrating T-cells in the DRG ranged from zero to 56 per 3 400x fields of view. DRG harboring latent VZV did not exhibit a significantly different number of T-cell infiltrates than those DRG without latent VZV (mean ± SEM for VZV-positive DRG = 19.2 ± 2.4; for VZV-negative DRG = 10.0 ± 2.7). The intensity of the T-cell infiltrates varied interindividually in the TG and DRG (Table 3). Overall, the TG contained significantly larger numbers of CD3+ T-cells than the DRG (Mann-Whitney U test, $p < 0.00001$; Fig. 2A).

Comparison of CD8 and RANTES in Trigeminal Ganglia versus Dorsal Root Ganglia From the Same Individuals

The expression of CD8 and RANTES was compared by quantitative RT-PCR in the TG and DRG of all but one individual included in this study (Fig. 2B, C). The high levels of CD8 transcripts in the TG were associated with high expression levels of the T-cell chemoattractant RANTES. In contrast, the DRG of the same individuals contained significantly fewer CD8 transcripts (Mann-Whitney U test, $p < 0.01$) and exhibited significantly lower levels of RANTES ($p < 0.001$; Fig. 2B). In a correlation analysis, induction factors for CD8 and RANTES correlated significantly in the TG versus DRG (Spearman rank order correlation, $r = 0.79$, $p < 0.001$; Fig. 2C), but there was no correlation between the amount of LAT and CD8 or RANTES transcripts.

Immunohistochemical RANTES staining revealed that RANTES was present only in the TG latently infected with HSV-1. A subpopulation of the infiltrating cells showed a cytoplasmic staining similar to that found in the positive tonsil control (Fig. 1G, H). No RANTES staining was found in the DRG latently infected with VZV (Fig. 1I). An overview of the distribution of viral latency markers and the presence of T-cells and RANTES in the TG versus DRG are shown for individual samples in Table 4.

DISCUSSION

In the current study, we showed that latent VZV in human DRG is in general not accompanied by a chronic inflammation. This is, however, consistently found in the TG latently infected with HSV-1 of the same individual. These findings suggest that HSV-1 is more effective than VZV in attracting T-cells into the peripheral nervous system despite the abundant occurrence of VZV protein 62 in many DRG and TG.

When using immunohistochemistry, we found that VZV protein 62 was evenly distributed between the TG and the DRG of the same individual (80% positive TG and 87% positive DRG). In contrast, LAT as a marker of HSV-1 latency was detected in only the TG. HSV-1 DNA could be amplified in 10 of 37 (27%) DRG only when nested PCR was applied. These findings confirm earlier studies on HSV-1 and VZV distribution (20–22).

Our data showed that the amount of expression of LAT does not correlate with the intensity of T-cell infiltration or RANTES production. Furthermore, T-cells were located mainly around LAT negative neurons (12). This indicates that other factors than LAT are responsible for attracting the T-cells. HSV-1 LAT genes are important for maintaining latency and promoting the survival of infected neurons (23). Very recently, it has been demonstrated that LAT exerts its antiapoptotic functions by downregulation of elements of the TGF-beta pathway through micro RNAs (24). This mechanism helps the virus to keep the host cell alive. The antiapoptotic activity of LAT may also play a role in counteracting the noxious effects of the CD8 cells.

However, evidence from the HSV-1 mouse model suggests that besides LAT, productive genes are also present during latency (7, 8, 25). Using very sensitive molecular techniques, we showed that the immediate–early genes ICP0 and ICP4 are also expressed during HSV-1 latency (Derfuss, unpublished data). It remains to be proven whether the protein of these immediate–early genes sustains the T-cell response in the TG. In the present study, we showed that abundant T-cells are only present in the TG and not in the DRG. This suggests that T-cells are attracted by HSV-1 but not by VZV.

The question arises as to why then HSV-1 and not VZV attracts T-cells. Although both viruses are neurotropic and can be found in the same ganglion and even in the same neuron (26, 27), the reactivation patterns of these 2 herpesviruses are completely different. These different reactivation

Notes to Table 4

VZV-positive neurons are given as a percentage of all neurons evaluated in 3 fields of view at a magnification of 400x. Between 20 and 120 neurons were analyzed for each ganglion. The relative amount of LAT transcript compared with GAPDH was analyzed using quantitative PCR. No LAT was detected in the DRG, whereas TG contained varying amounts of LAT. The third column shows results of the nested HSV-1 DNA PCR.

The second part of the table indicates parameters of the immune response for the respective ganglia. CD3+ T-cells were counted in 3 fields of view at a magnification of 400x in fields containing clusters or groups of T-cells. CD8 relative transcript number and RANTES relative transcript numbers were determined for most ganglia using quantitative reverse transcriptase–PCR.

VZV, varicella zoster virus; LAT, latency-associated transcript; HSV-1, herpes simplex virus type 1; ND, not done; PCR, polymerase chain reaction.

patterns may help to explain the apparent paradox that a latent virus infection with abundant protein expression (e.g., VZV) is hiding from the host's immune system, whereas latent HSV-1 infection, which apparently shows no detectable protein during latency, induces a strong immune response. It is conceivable that repeated reactivations of HSV-1 produce a strong immunogenic stimulus that continues throughout the periods of viral latency. During reactivation, this inflammatory milieu could induce major histocompatibility complex class I expression on neurons, which enables the neurons to present viral antigen to the surrounding T-cells. Conversely, the absence of an inflammatory milieu in cases of latent VZV, which only rarely reactivates, would render the virus invisible to the T-cells. A possible mechanism by which this can be accomplished is the blocking of antigen presentation by VZV protein. This has been demonstrated in cell cultures acutely infected with VZV (28).

The role of the T-cells in latent HSV-1 infection remains unclear. Infiltrating T-cells could inhibit repeated reactivation of the virus, prevent viral spread to the central nervous system, or support the infected neurons by secreting a neurotrophic factor. On the other hand, the T-cells could be just a bystander effect of a recurrent reactivation, having no major impact on viral latency. The high transcript levels of the chemoattractant RANTES and its presence at the protein level only found in the TG argue against this latter possibility. In the DRG, the transcripts levels of RANTES were lower than in the TG. No RANTES protein was present in the DRG, indicating that there was no active inflammation. In vivo experiments demonstrated that the expression of RANTES could be induced through a mechanism dependent on *ICP0* (29). It is interesting that VZV does not possess an equivalent of the HSV-1 *ICP0* gene (30). Moreover, *ICP0* is the only gene needed to induce reactivation of HSV-1 (31). One could speculate that the difference in the pathogenesis of HSV-1 and VZV originates at the level of the immediate–early genes and the immune response against them. We have illustrated the possible mechanisms by which latent HSV-1 and VZV are regulated in TG and DRG (Fig. 3).

The difference in the immune response to latent HSV-1 and VZV reflects the complex interplay between

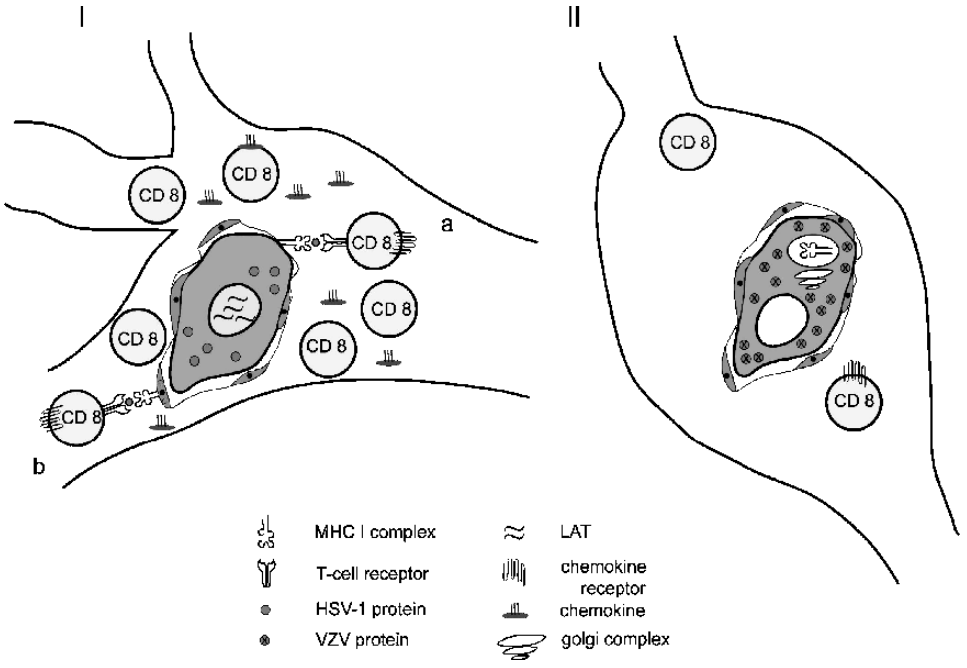

FIGURE 3. Schematic representation of the putative processes through which latent herpes simplex virus type 1 (HSV-1) initiates an immune response in the trigeminal ganglia (TG) and through which latent varicella zoster virus (VZV) evades the immune response in dorsal root ganglia (DRG). (*I*) CD8+ T-cells are recruited to TG latently infected with HSV-1 by chemokines like RANTES. HSV-1-specific CD8+ T-cells are activated through their antigen-specific T-cell receptor. In this context, 2 different types of antigen presentation are conceivable: (a) major histocompatibility complex (MHC) I expression is induced on the sensory neurons through the inflammatory milieu so that the neurons themselves are able to present viral peptides through their own MHC I complex to antigen-specific CD8+ T-cells. (b) In a different model, antigenic viral peptide is transferred from latently infected neurons to satellite glia cells, which present the peptide on their MHC I complex to the antigen-specific CD8+ T-cells. (*II*) In DRG latently infected with VZV, the presentation of the abundant intracellular viral protein on the neural surface is inhibited by the MHC I complex being retained in the Golgi compartment. The lack of surface expression of MHC I could also be the result of the "noninflammatory milieu" resulting from the rare VZV reactivation frequency. Hence, latent VZV protein is not presented at the cell surface and cannot be recognized by the few T-cells that enter the VZV latently infected DRG.

herpes viral products and components of the acquired immune system and becomes manifest in the different frequencies of reactivation of both viruses. Obviously, the immune cells and HSV-1 coevolved over millions of years during which they established a perfect equilibrium with minimal damage to either. If we could decipher this relationship, we would know more about the normal human immune system (32).

ACKNOWLEDGMENTS

The authors thank Dr. Hendricks, University of Pittsburgh, for helpful suggestions and fruitful discussions; Igor Paripovic for technical assistance; Sabine Esser for preparing Figure 3; and Judy Benson for carefully copy-editing the manuscript.

REFERENCES

1. Meier JL, Straus SE. Comparative biology of latent varicella-zoster virus and herpes simplex virus infections. J Infect Dis 1992;166 (suppl 1): S13–23
2. Mitchell BM, Bloom DC, Cohrs RJ, et al. Herpes simplex virus-1 and varicella-zoster virus latency in ganglia. J Neurovirol 2003;9:194–204
3. Arvin AM. Varicella-zoster virus. Clin Microbiol Rev 1996;9:361–81
4. McGeoch DJ, Cook S, Dolan A, et al. Molecular phylogeny and evolutionary timescale for the family of mammalian herpesviruses. J Mol Biol 1995;247:443–58
5. Wagner EK, Bloom DC. Experimental investigation of herpes simplex virus latency. Clin Microbiol Rev 1997;10:419–43
6. Kang W, Mukerjee R, Fraser NW. Establishment and maintenance of HSV latent infection is mediated through correct splicing of the LAT primary transcript. Virology 2003;312:233–44
7. Feldman LT, Ellison AR, Voytek CC, et al. Spontaneous molecular reactivation of herpes simplex virus type 1 latency in mice. Proc Natl Acad Sci U S A 2002;99:978–83
8. Kramer MF, Chen SH, Knipe DM, et al. Accumulation of viral transcripts and DNA during establishment of latency by herpes simplex virus. J Virol 1998;72:1177–85
9. Lungu O, Panagiotidis CA, Annunziato PW, et al. Aberrant intracellular localization of varicella-zoster virus regulatory proteins during latency. Proc Natl Acad Sci U S A 1998;95:7080–85
10. Grinfeld E, Kennedy PG. Translation of varicella-zoster virus genes during human ganglionic latency. Virus Genes 2004;29:317–19
11. Croen KD. Varicella-zoster virus latency. Annu Rev Microbiol 1991; 45:265–82
12. Theil D, Derfuss T, Paripovic I, et al. Latent herpesvirus infection in human trigeminal ganglia causes chronic immune response. Am J Pathol 2003;163:2179–84
13. Liu T, Khanna KM, Chen X, et al. CD8(+) T cells can block herpes simplex virus type 1 (HSV-1) reactivation from latency in sensory neurons. J Exp Med 2000;191:1459–66
14. Khanna KM, Bonneau RH, Kinchington PR, et al. Herpes simplex virus-specific memory CD8+ T cells are selectively activated and retained in latently infected sensory ganglia. Immunity 2003;18:593–603
15. Swanson BJ, Murakami M, Mitchell TC, et al. RANTES production by memory phenotype T cells is controlled by a posttranscriptional, TCR-dependent process. Immunity 2002;17:605–15
16. Aurelius E, Johansson B, Skoldenberg B, et al. Rapid diagnosis of herpes simplex encephalitis by nested polymerase chain reaction assay of cerebrospinal fluid. Lancet 1991;337:189–92
17. Theil D, Arbusow V, Derfuss T, et al. Prevalence of HSV-1 LAT in human trigeminal, geniculate, and vestibular ganglia and its implication for cranial nerve syndromes. Brain Pathol 2001;11:408–13
18. Lynas C, Cook SD, Laycock KA, et al. Detection of latent virus mRNA in tissues using the polymerase chain reaction. J Pathol 1989;157:285–89
19. Naoe M, Marumoto Y, Ishizaki R, et al. Correlation between major histocompatibility complex class I molecules and CD8+ T lymphocytes in prostate, and quantification of CD8 and interferon-gamma mRNA in prostate tissue specimens. BJU Int 2002;90:748–53
20. Mahalingam R, Wellish M, Wolf W, et al. Latent varicella-zoster viral DNA in human trigeminal and thoracic ganglia. N Engl J Med 1990; 323:627–31
21. Mahalingam R, Wellish MC, Dueland AN, et al. Localization of herpes simplex virus and varicella zoster virus DNA in human ganglia. Ann Neurol 1992;31:444–48
22. Mahalingam R, Wellish M, Lederer D, et al. Quantitation of latent varicella-zoster virus DNA in human trigeminal ganglia by polymerase chain reaction. J Virol 1993;67:2381–84
23. Perng GC, Jones C, Ciacci-Zanella J, et al. Virus-induced neuronal apoptosis blocked by the herpes simplex virus latency-associated transcript. Science 2000;287:1500–503
24. Gupta A, Gartner JJ, Sethupathy P, et al. Anti-apoptotic function of a microRNA encoded by the HSV-1 latency-associated transcript. Nature 2006;442:82–85
25. Decman V, Kinchington PR, Harvey SA, et al. Gamma interferon can block herpes simplex virus type 1 reactivation from latency, even in the presence of late gene expression. J Virol 2005;16:10339–47
26. Theil D, Derfuss T, Strupp M, et al. Cranial nerve palsies: Herpes simplex virus type 1 and varicella-zoster virus latency. Ann Neurol 2002;51: 273–74
27. Theil D, Paripovic I, Derfuss T, et al. Dually infected (HSV-1/VZV) single neurons in human trigeminal ganglia. Ann Neurol 2003;54:678–81
28. Abendroth A, Lin I, Slobedman B, et al. Varicella-zoster virus retains major histocompatibility complex class I proteins in the Golgi compartment of infected cells. J Virol 2001;75:4878–88
29. Melchjorsen J, Pedersen FS, Mogensen SC, et al. Herpes simplex virus selectively induces expression of the CC chemokine RANTES/CCL5 in macrophages through a mechanism dependent on PKR and ICP0. J Virol 2002;76:2780–88
30. Davison DJ, McGeoch DJ. Evolutionary comparisons of the S segments in the genomes of herpes simplex virus type 1 and varicella-zoster virus. J Gen Virol 1986;67:597–611
31. Russell J, Stow ND, Stow EC, Preston CM. Herpes simplex virus genes involved in latency in-vitro. J Gen Virol 1987;68:3009–18
32. Zinkernagel RM. Immunology taught by viruses. Science 1996;271: 173–78

